Chromosomal-level genome of the *Pinus massoniana* 'Minlin WY36'

Wei-Hong Sun[1,2*], Feiping Zhang[2*], Xuewei Zhao[1,2*], Zhen Li[3*], Ke-Wei Liu[4*], Songqing Wu[2], Yajie Guo[2], Xia Hu[2], Mengyao Zeng[1], Linying Wang[1], Cheng-Yuan Zhou[1,2], Deqiang Chen[1,2], Ruiyue Zheng[1], Xiaopei Wu[1], Dong-Hui Peng[1,2], Liang Ma[1], Zhi-Wen Wang[5], Wenfeng Lan[6], Huimin Chen[6], Shuangquan Zou[1,2†], Wen-Chieh Tsai[1,7,8†], Yves Van de Peer[3,9,10†], Zhong-Jian Liu[1,2†], Siren Lan[1,2†]

1. Key Laboratory of National Forestry and Grassland Administration for Orchid Conservation and Utilization at College of Landscape Architecture and Art, Fujian Agriculture and Forestry University, Fuzhou 350002, China

2. Fujian Colleges and Universities Engineering Research Institute of Conservation and Utilization of Natural Bioresources, College of Forestry, Fujian Agriculture and Forestry University, Fuzhou 350002, China

3. Department of Plant Biotechnology and Bioinformatics, Ghent University, 9052 Ghent, Belgium

4. Tsinghua-Berkeley Shenzhen Institute (TBSI), Center for Biotechnology and Biomedicine, Shenzhen Key Laboratory of Gene and Antibody Therapy, State Key Laboratory of Chemical Oncogenomics, State Key Laboratory of Health Sciences and Technology, Institute of Biopharmaceutical and Health Engineering (iBHE), Shenzhen International Graduate School, Tsinghua University, Shenzhen 518055, China

5. PubBio-Tech, Wuhan 430070, China

6. Wuyi Forestry Farm of Fujian, Zhangping 364400, China

7. Institute of Tropical Plant Sciences and Microbiology, National Cheng Kung University, Tainan 701, Taiwan

8. Orchid Research and Development Center, National Cheng Kung University, Tainan City 701, Taiwan

9. College of Horticulture, Nanjing Agricultural University, Academy for Advanced

Interdisciplinary Studies, Nanjing 210095, China

10. Centre for Microbial Ecology and Genomics, Department of Biochemistry, Genetics and Microbiology, University of Pretoria, Pretoria, South Africa

*These authors contributed equally to this work.

†Correspondence and requests for materials should be addressed to S. Z. (zou@fafu.edu.cn), W.-C. T. (tsaiwc@mail.ncku.edu.tw), Y. V. d. P. (yves.vandepeer@psb.vib-ugent.be), Z-J. L. (zjliu@fafu.edu.cn) or S. L. (lkzx@fafu.edu.cn).

Abstract

Owing to conifers complex and large genomes, it is challenging to construct a comprehensive reference genome and conduct evolutionary and genomic research. Here, we present the chromosome-level assembly of *Pinus massoniana* 'Minlin WY36', a pioneering conifer species used for afforestation, timber production, and oleoresin extraction. The genome size was determined to be 23.41 Gb, with a contig N50 value of 1.15 Mb and a scaffold N50 value of 2.02 Gb. A total of 23.16 Gb of reads (98.93% of the assembled genome) were anchored and oriented onto 12 pseudochromosomes, with chromosome lengths from 1.47 to 2.29 Gb. A total of 32,144 protein-coding genes were predicted, of which 27,173 (84.54%) were functionally annotated. The *P. massoniana* 'Minlin WY36' genome consists of 79.41% (18.57 Gb) repetitive sequences, among which long terminal repeat sequences (LTR) were the most abundant. Through comparative genomic analysis, we found that the unique and significantly expanded genes in *P. massoniana* 'Minlin WY36' were enriched in the metabolism related to resin synthesis. This study offers valuable insights into conifer evolution and contributes resources for further investigations of conifer adaptation and developmental processes.

Introduction

Pines (genus *Pinus*) belong to the coniferous family Pinaceae of gymnosperms, with approximately 110–120 species distributed across the Northern Hemisphere (Gernandt *et al.*, 1999). Among these, *Pinus massoniana* is a unique conifer species endemic to China (He *et al.*, 2023). Its planting area ranks first in the distribution of tree species in China, and is widely distributed in southern China. As a crucial species for afforestation, timber production, and oleoresin extraction, *P. massoniana* has extensive applications in construction, papermaking, and pharmaceutical industries and has important ecological and economic significance (Peng *et al*. 2003; Zhang *et al*. 2013). In this study, we generated a high-quality *P. massoniana* 'Minlin WY36' genome sequence to elucidate the evolution of its genome structure and phylogenetic relationships within gymnosperms. This study offers profound insights into the evolution of conifers and serves as a foundation for the further exploration of their adaptive developmental strategies.

Results and discussion

Survey analysis revealed a high level of heterozygosity in the *P. massoniana* 'Minlin WY36' genome, accounting for 1.13% of the 23.38 Gb genome size determined by *K*-mer analysis. For *de novo* whole-genome sequencing of *P. massoniana* 'Minlin WY36', we obtained 2165.08 Gb of clean reads with an average length of 12.47 Kb using PacBio technology. The final assembled genome amounted to 25.37 Gb with a contig N50 value of 1.15 Mb (**Table 1**). High-throughput and high-resolution chromosome conformation capture (Hi-C) technology was used to obtain a chromosome-level genome. Based on the Hi-C data, the genome was assembled to a total size of 23.41 Gb with a scaffold N50 value of 2.02 Gb (**Table 1**). A total of 23.16 Gb reads were mapped to 12 chromosomes, with the chromosome lengths ranging from 1.47 to 2.29 Gb (**Table 2**).

To predict gene models, we used a combination of *de novo* prediction, homology-based searches, and RNA-sequencing data, resulting in the prediction of 32,144 protein-coding genes in *P. massoniana* 'Minlin WY36' genome. The primary gene models exhibited a mean length of 37,832.39 bp, with an average exon length of 263.80 bp and an average intron length of 12,804.88 bp. Similar to other gymnosperms with large genomes, extremely long introns were also predicted in *P. massoniana* 'Minlin WY36' (**Figure 1A**). This indicates that the accumulation of long introns has led to a significant expansion of the genome (Nystedt *et al.*, 2013). On the basis of a

83 Benchmarking Universal Single-Copy Orthologs (BUSCO) assessment, the completeness of the
84 gene annotations was approximately 81.75%. We functionally annotated the protein-coding genes
85 using various databases, including Gene Ontology (GO), Kyoto Encyclopedia of Genes and
86 Genomes (KEGG), Swiss-Prot, and others, an over 84.54% of the genes could be mapped to
87 corresponding functional items. These analyses indicate a relatively comprehensive structural
88 annotation of the reference genome. A total of 113 microRNAs (miRNAs), 730 small nuclear
89 RNA (snRNAs), 2,011 transfer RNAs (tRNAs), and 3,307 ribosomal RNAs (rRNA) were
90 identified in the *P. massoniana* 'Minlin WY36' genome (**Table 3**). We estimated that 79.41%
91 (18.57 Gb) of the *P. massoniana* genome was composed of repetitive sequences, among which
92 transposable elements (TE) sequences were relatively abundant, with a long terminal repeat (LTR)
93 accounting for 70.94%, followed by LINE accounting for 4.88%, and DNA accounting for 2.34%.
94 We used complete LTR-Copia and LTR-Gypsy elements from *P. massoniana* 'Minlin WY36' to
95 investigate further the timing of conifer transposable element insertions and found that insertions
96 appear to have occurred tens of millions of years ago (**Figure 1B**).
97 The phylogenetic relationships among the major lineages of existing gymnosperms, particularly
98 Ginkgo and Gnetales, remain a subject of ongoing debate (Stull *et al*., 2021). On the basis of the
99 46 low-copy gene families derived from ten gymnosperms, five angiosperms, and five seedless
100 vascular plants, we constructed phylogenetic tree (**Figure 1C**). The results support Gnetales as a
101 basal lineage within gymnosperms, diverging from other gymnosperms approximately 249.7
102 million years ago (Mya). *Ginko biloba* and *Cycas panzhihuaensis* form a sister group to conifers,
103 with these two major evolutionary branches diverging around 177.3 Mya. *Taxus wallichiana* –
104 *Cunninghamia lanceolata* diverged from Pinaceae approximately 160.4 Mya. Approximately 51
105 Mya, Pinaceae rapidly diversified into other species, and *P. massoniana* 'Minlin WY36' diverged
106 around 12.6 Mya.
107 A comparative analysis of orthologous genes among *P. massoniana* 'Minlin WY36' and the
108 genomes of 19 species revealed that 1,011 gene families (including 3,074 genes) were unique to
109 the *P. massoniana* 'Minlin WY36' genome. Enrichment analyses found that these genes are
110 especially enriched in the Kyoto Encyclopedia of Genes and Genomes (KEGG) terms of 'plant-
111 pathogen interaction', 'Flavonoid biosynthesis', 'isoflavanoid biosynthesis', 'Fatty acid
112 biosynthesis', and 'Fatty acid degradation', 'Fatty acid elongation' (**Figure 1D**). Analysis of

113 orthologous gene family expansion and contraction indicated 2,022 expanded gene families in the
114 *P. massoniana* 'Minlin WY36' genome, of which 370 (including 3,868 genes) exhibited
115 significant expansion ($P<0.01$). Additionally, 467 gene families were contracted, with 108 gene
116 families (including 663 genes) showing a significant contraction (**Figure 1C**). Enrichment
117 analyses revealed that the significantly expanded gene families were enriched the KEGG
118 pathways related to 'terpenoid backbone biosynthesis', 'diterpenoid biosynthesis', 'flavone and
119 flavonol biosynthesis', and 'plant-pathogen interaction', 'fatty acid degradation' (**Figure 1E**).
120 Resin is a major metabolite of pine plants and serves as a physical and chemical defense barrier
121 against insect and pathogen attacks (Liu *et al.*, 2021). Resin mainly consist of terpenoids,
122 flavonoids, lignin-like compounds, and phenolic compounds, among which terpenoids are the
123 predominant components (Li *et al.*, 2013). The genes that are specific and significantly expanded
124 in *P. massoniana* 'Minlin WY36' are enriched in pathways related to plant-pathogen interactions,
125 terpenoid metabolism, and flavonoid metabolism.
126

127 **Methods**

128 **DNA extraction and sequencing**

129 All genome-sequencing materials used in this study were collected from adult *P. massoniana*
130 'Minlin WY36' grown in Youxi County, Fujian Province, China. Total genomic DNA was
131 extracted from young leaves using the cetyltrimethylammonium bromide method (CTAB) for
132 Illumina and PacBio sequencing. We used the PacBio Sequel II platform to perform 26-cell single-
133 molecule real-time DNA sequencing.
134

135 **Genome size estimate**

136 Before genome assembly, filtered Illumina reads were used to estimate the genome size,
137 heterozygosity, and repeat content of *P. massoniana* 'Minlin WY36'. Then, a genome survey was
138 performed through *K*-mer analysis using Jellyfish v2.1.4 (Marçais and Kingsford, 2011) and
139 GenomeScope (Vurture *et al*., 2017).
140

141 **Genome assembly and Hi-C scaffolding**

142 Assemble *P. massoniana* 'Minlin WY36' genome using PacBio data. Canu v1.9

143 (https://github.com/marbl/canu) (Koren *et al*., 2017) was used to correct the error of the PacBio
144 clean data. We assembled the corrected data using Smartdenovo v1.0 (Ruan, 2016). The Contig-
145 level assembly results were aligned to the genome using Juicer (Kent, 2002), and the alignment
146 results were filtered to remove incorrectly aligned reads. Next, 3D-DNA (Ruan, 2016) was used to
147 perform preliminary clustering, ordering, and orientation of the genomic sequences. To prevent
148 excessive fragmentation of the genomic sequences, we manually adjusted the preliminary
149 clustering results from 3D-DNA using visualization software Juicebox
150 (https://github.com/aidenlab/Juicebox). This manual adjustment involved removing redundancies,
151 repositioning, and re-clustering, as necessary. The final pseudochromosomes were manually
152 constructed and adjusted. To evaluate the results of the Hi-C assembly, we constructed an
153 interaction heat map of Hi-C assembly chromosome.
154

155 **Gene prediction and annotation**

156 Annotation information from five closely related species (*Amborella trichopoda*, *G. biloba*, *G.*
157 *monatum*, *P. abies*, and *P. taeda*) was used for homology-based predictions. From the structurally
158 intact genes obtained through homology-based prediction, we randomly selected 5,000 genes to
159 train the de novo models of the target species using the ab initio prediction software, Augustus and
160 SNAP (Johnson *et al*., 2008). Simultaneously, the RNA-seq data were aligned to the genome using
161 HISAT v2.1.0 (Kim *et al*., 2015) and the resulting transcripts were assembled using StringTie
162 v1.3.4d (Pertea *et al*., 2015). Finally, Maker v2.31.8 (Holt and Yandell, 2011) software was used to
163 integrate homology-based predictions. In addition, the gene sets obtained from gene structure
164 annotation were aligned with known protein databases and other databases such as SwissProt
165 (Boeckmann, 2005) (http://www.uniprot.org/), TrEMBL (http://www.uniprot.org/) (Boeckmann,
166 2005), KEGG (Kanehisa and Goto, 2000) (http://www.genome.jp/kegg/), and InterPro
167 (https://www.ebi.ac.uk/interpro/) (Zdobnov and Apweiler, 2001) and were aligned using Blast
168 v2.2.26 (Altschul *et al*., 1990).
169

170 **Identification of non-coding RNA, and repetitive sequences**

171 Non-coding RNAs include RNA with a variety of known functions, such as microRNAs
172 (miRNAs), ribosomal RNA (rRNA), and transfer RNA (tRNA). Based on the structural

173 characteristics of tRNA, software tRNAscan-SE 1.3.1 (http://lowelab.ucsc.edu/tRNAscan-SE/)
174 (Lowe and Eddy, 1997) was used to search for tRNA sequences in the genome. Owing to the high
175 conservation of rRNA, rRNA sequences from closely related species was selected as reference
176 sequences, and BLASTN alignment was used to search for rRNA sequences in the genome.
177 Additionally, covariance models from the Rfam family (Sam *et al*., 2005), along with the
178 INFERNAL software (http://infernal.janelia.org/) provided by Rfam, can be used to predict
179 miRNA and snRNA sequence information in the genome.
180 The process involved identifying sequences similar to known repetitive sequences based on the
181 RepBase v21.12 (Jurka *et al*., 2005) database (http://www.girinst.org/repbase) using
182 RepeatMasker v4.0.7 (http://www.repeatmasker.org) and RepeatProteinMask v4.0.7
183 (http://www.repeatmasker.org). *De novo* prediction, on the other hand, is based on self-sequence
184 alignment, where a *de novo* (Price *et al.*, 2005) repetitive sequence library was first established
185 using RepeatModeler (http://www.repeatmasker.org) and LTR_FINDER v1.06
186 (http://tlife.fudan.edu.cn/ltr_) (Benson, 1997). This library was then used for prediction using the
187 RepeatMasker software. Additionally, Tandem Repeats Finder v4.09
188 (http://tandem.bu.edu/trf/trf.html) (Price *et al*., 2005) was used to search for tandem repeats within
189 the genome.
190

191 **Ortholog detection**

192 Single/low-copy and multicopy gene families can be obtained by identifying orthologous genes
193 and cluster analysis of gene families. A protein dataset that included ten gymnosperms, five
194 angiosperms, and five seedless vascular plants was constructed. Pairwise BLASTP (Altschul *et*
195 *al*., 1990) alignments were performed on the protein dataset, followed by a clustering analysis
196 using OrthoFinder (Emms and Kelly, 2015).
197

198 **Phylogenetic reconstruction**

199 We constructed a species phylogenetic tree using low-copy gene families from *P. massoniana*
200 'Minlin WY36' and 19 other plants and identified 46 low-copy families among the 20 species.
201 Then, the dataset used for phylogenetic analysis was employed in the MCMCTree program within
202 PAML4.9 (Ziheng, 2007) to estimate the divergence times. The nucleotide substitution model was

set as the GTR model and the molecular clock model was set as the independent rate model. The MCMC process included 500,000 burn-in iterations and 1,500,000 sampling iterations, with sampling conducted every 150 iterations. The same parameters were run twice to obtain stable results. The phylogeny was calibrated using various fossil records or molecular divergence estimates by placing soft bounds on the split nodes of *G. montanum* – *G. biloba* (230–282 Ma), *Arabidopsis thaliana* – *G. montanum* (289–330 Ma), *Azolla pinnata* – *A. thaliana* (392–422 Ma), and *Physcomitrella patens* – *A. thaliana* (465–533 Ma).

Gene family expansion and contraction

For the well-clustered gene families and the constructed phylogenetic tree structures, we performed gene family contraction and expansion analysis on the selected 20 species using CAFÉ 4 (De Bie *et al*., 2006). We conducted KEGG and GO enrichment analyses focusing on genes belonging to the notably expanded gene family within the *P. massoniana* 'Minlin WY36' genome.

Acknowledgments

This project was supported by the Forestry Peak Discipline Construction Project of Fujian Agriculture and Forestry University **(72202200205)**, the National Key Research and Development Program of China **(No. 2203YFD1600504)**, and Fujian Forestry Science and Technology Program **(No.2020-9)**.

Competing interests

The authors declare no competing interests.

Reference

Altschul, S. F. *et al*. Basic local alignment search tool. *Journal of Molecular Biology* 215(3): 403–410 (1990).

Benson, G. Tandem repeats finder: a program to analyze DNA sequences. *Nucleic Acids Research* 27(2): p. 573–580 (1997).

Boeckmann, B. *et al*. The SWISS-PROT protein knowledgebase and its supplement TrEMBL in 2003. *Nucleic Acids Research* 1(1): p. 365–370 (2003).

De Bie, T. *et al*. CAFE: a computational tool for the study of gene family evolution. *Bioinformatics* 22(10): 1269–1271 (2006).

Emms, D. and Kelly, S. OrthoFinder: solving fundamental biases in whole genome comparisons dramatically improves orthogroup inference accuracy. *Genome Biology* 16: 157 (2015).

Gernandt, D.S. *et al.* Molecular phylogeny of Pinaceae and *Pinus*. *In IV International Conifer Conference* 615:107–114 (1999).

He, Y. *et al.* Potential geographical distribution and its multi-factor analysis of Pinus massoniana in China based on the maxent model. *Ecological Indicators* 154: 110790 (2023).

Holt, C. and Yandell, L. MAKER2: an annotation pipeline and genome-database management tool for second-generation genome projects. *BMC Bioinformatics* 12(1): p. 491 (2011).

Johnson, A.D. *et al.* SNAP: a web-based tool for identification and annotation of proxy SNPs using HapMap. *Bioinformatics* 24(24): 2938–2939 (2008).

Jurka, J. *et al.* Repbase Update, a database of eukaryotic repetitive elements. *Cytogenet Genome Res.* 110(1–4): 462–7 (2005).

Kanehisa, M. and Goto, S. KEGG: kyoto encyclopedia of genes and genomes. *Nucleic Acids Research* 28(1): p. 27–30 (2000).

Kent, W. J. BLAT-the BLAST-like alignment tool. *Genome Research* 12, 656–664 (2002).

Kim, D. *et al.* HISAT: a fast spliced aligner with low memory requirements. *Nature Methods* 12(4): 357 (2015).

Koren, S. *et al.* Canu: scalable and accurate long-read assembly via adaptive k-mer weighting and repeat separation. *Genome Research* 27: 722–736 (2017).

Li, B. *et al.* Chemical constituents and biological activities of Pinus species. *Chemistry & Biodiversity* 10(12): 2133–2160 (2013)

Liu, B. *et al.* Two terpene synthases in resistant Pinus massoniana contribute to defence against Bursaphelenchus xylophilus. *Plant Cell Environ.* 44: 257–274 (2021).

Lowe, T. M. and Eddy, S. R. tRNAscan-SE: a program for improved detection of transfer RNA genes in genomic sequence. *Nucleic Acids Research* 25(5): 955–964 (1997).

Marçais, G. and Kingsford, C. A fast, lock-free approach for efficient parallel counting of occurrences of k-mers. *Bioinformatics* 27(6): 764–770 (2011).

Nystedt, B. *et al.* The *Norway spruce* genome sequence and conifer genome evolution. *Nature* 497: 579–584 (2013).

Peng, S. L. *et al.* Genetic diversity of *Pinus massoniana* revealed by RAPD markers. *Silvae Genetica* 52(2): 60–63 (2003).

Pertea, M. *et al.* StringTie enables improved reconstruction of a transcriptome from RNA-seq reads. *Nature Biotechnology* 33(3): 290 (2015).

Price, A. L. *et al.* De novo identification of repeat families in large genomes. *Bioinformatics* 21 (suppl_1): p. i351 (2005).

Stamatakis A. RAxML Version 8: A tool for phylogenetic analysis and post analysis of large phylogenies. *Bioinformatics* 30 (9): 1312–1313. 6 (2014).

Ruan, J. Ultra-fast de novo assembler using long noisy reads. Available at https://github.com/ruanjue/smartdenovo (2016).

Sam, G. J. *et al.* Rfam: annotating non-coding RNAs in complete genomes. *Nucleic Acids Res* 33, 121–124 (2005).

Stull, G.W. *et al.* Gene duplications and phylogenomic conflict underlie major pulses of phenotypic evolution in gymnosperms. *Nature Plants* 7: 1015–1025 (2021).

Vurture, G. W. *et al.* GenomeScope: fast reference-free genome profiling from short reads. *Bioinformatics* 33, 2202–2204 (2017).

Zdobnov, E. and Apweiler, R. InterProScan--an integration platform for the signature-recognition methods in InterPro. *Bioinformatics* 17(9): p. 847–848 (2001).

Zhang, Y. *et al.* Divergence among Masson pine parents revealed by geographical origins and SSR markers and their relationships with progeny performance. *New Forests* 44(3): 341–355 (2013).

Ziheng, Y. PAML 4: phylogenetic analysis by Maximum Likelihood. *Molecular Biology and Evolution* 24(8):1586–1591 (2007).

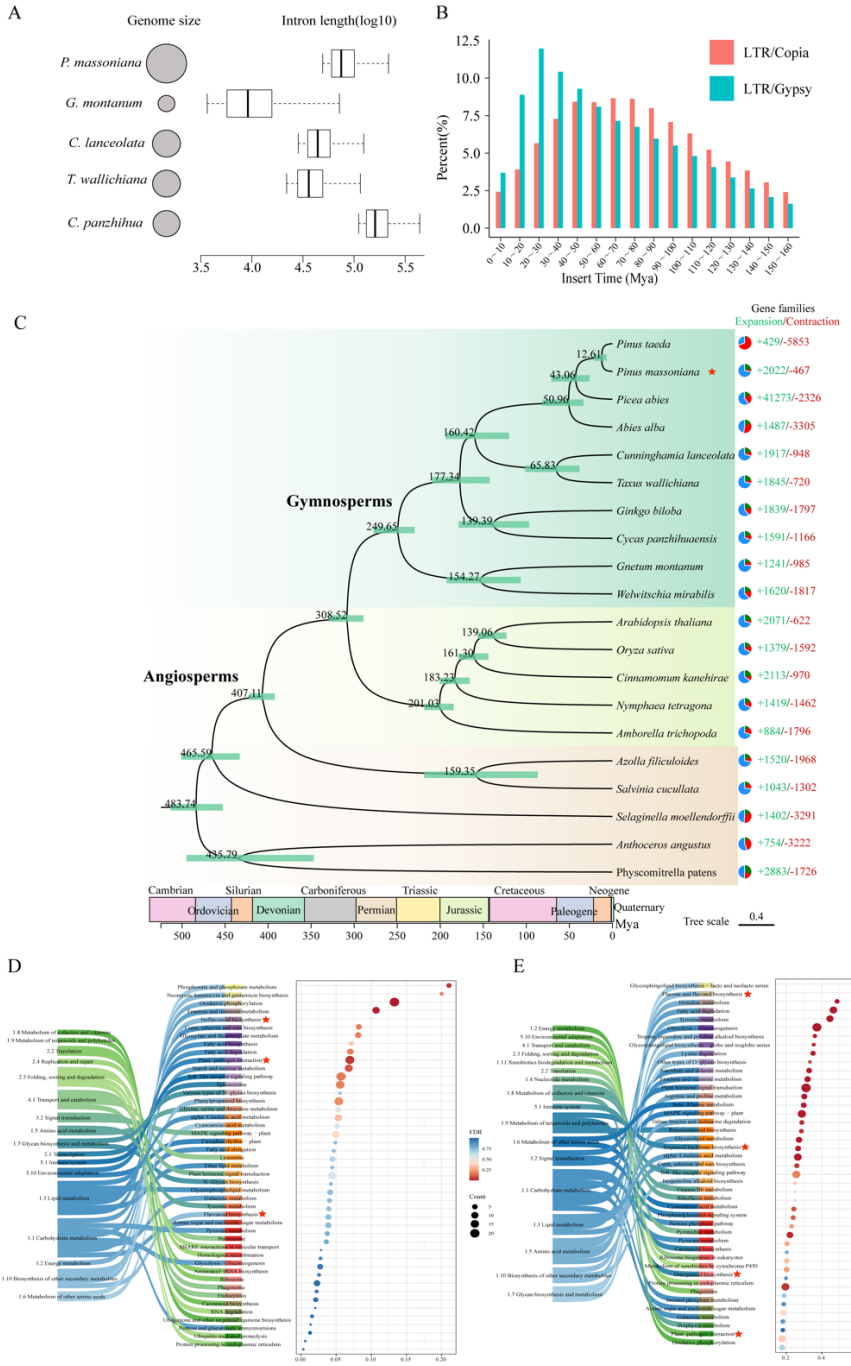

Figure 1. Assembly and genome features of *Pinus massoniana*. A. Intron length. **B.** Long terminal repeat insertion time in *P. massoniana* 'Minlin WY36'. **C.** Phylogenetic tree showing divergence times and evolution of the gene family size in the 20 species. Green and red numbers indicate the number of expanded and contracted gene families, respectively. The blue portions of the pie charts represent gene families with constant copy number. **D**. KEGG enrichment of genes unique to *P. massoniana* 'Minlin WY36'. **E**. KEGG enrichment of significantly expanded genes in *P. massoniana* 'Minlin WY36'.

295 **Table 1. The statistic of genome assembly of *P. massoniana* 'Minlin WY36'**

	PacBio		Hi-C			
	Contig		Contig		Scaffold	
	Length (bp)	number	Length (bp)	number	Length (bp)	number
N10	3,724,787	511	3,833,550	464	2,123,896,708	2
N20	2,622,261	1,339	2,717,123	1,203	2,097,736,443	3
N30	1,970,160	2,461	2,083,964	2,192	2,062,774,537	4
N40	1,504,588	3,942	1,617,216	3,472	2,044,626,210	5
N50	1,148,364	5,877	1,260,099	5,112	2,022,513,744	6
N60	857,477	8,433	976,522	7,217	1,994,193,789	7
N70	610,192	11,937	731,502	9,986	1,962,048,899	8
N80	401,083	17,049	515,242	13,788	1,679,226,079	10
N90	217,481	25,535	314,617	19,528	1,602,319,435	11
Longest	11,613,428	-	11,613,428	-	2,294,541,500	-
Total Length	25,367,207,913	-	23,390,460,802	-	23,407,722,302	-
GC Rate	0.381	-	0.381	-	0.381	-

296

297 **Table 2. The length of chromosome by Hi-C assemble of *P. massoniana* 'Minlin WY36'**

Chromosome ID	Length (bp)
Chr01	2,294,541,500
Chr02	2,097,736,443
Chr03	2,022,513,744
Chr04	1,472,222,046
Chr05	2,123,896,708
Chr06	1,994,193,789
Chr07	2,062,774,537
Chr08	2,044,626,210
Chr09	1,602,319,435
Chr10	1,679,226,079
Chr11	1,807,631,255
Chr12	1,962,048,899

298

299 **Table 3. Statistics on the annotation of non-coding RNA of the *P. massoniana* 'Minlin**

300 **WY36'genome.**

Type		Copy	Average length (bp)	Total length (bp)
	miRNA	113	136.54	15,429
	tRNA	2,011	74.59	150,009
rRNA	rRNA	3,307	678.98	2,245,395
	18S	1,070	1815.11	1,942,172
	28S	519	202.94	105,328
	5.8S	148	157.93	23,374
	5S	1,570	111.16	174,521
snRNA	snRNA	730	123.78	90,363
	CD-box	73	127.15	9,282
	HACA-box	28	115.75	3,241
	splicing	629	123.75	77,840

301